Thermochimica Acta 386 (2002) 43–49

thermochimica acta

www.elsevier.com/locate/tca

The decomposition kinetics of the SiO_2 coated nano-scale calcium carbonate

Miao Shui, Linhai Yue, Yimiao Hua, Zhude Xu*

Department of chemistry, Zhejiang University, Hangzhou 310027, PR China

Received 22 May 2001; received in revised form 7 August 2001; accepted 28 August 2001

Abstract

The model-free and model fitting approaches have been applied to the data for non-isothermal decomposition kinetics of SiO_2 surface coated calcium carbonate as well as the reference. The decomposition mechanisms as revealed by computation show great differences. Nano-sized reference samples decompose according to the contracting volume mechanism (R_3) while the surface SiO_2 coated calcium carbonate shows the one-dimensional diffusion (D_1) behavior, possibly because of the framework constituted by surface SiO_2 layer hinders the diffusion of the dissociate products into the outer atmosphere. At the mean time, the activation energy is increased by 30–35 kJ/mol in the process controlled by diffusion compared with the reference. However, the usual model fitting approach may also yield highly uncertain values of Arrhenius parameters when applied to non-isothermal data, so that a combination of master plot method and model-free kinetic approaches based on the isoconversional method that yields the dependencies of the activation energy on the extent of the conversion were also used to evaluate the credulity of the kinetic parameters achieved by model fitting methods. © 2002 Elsevier Science B.V. All rights reserved.

Keywords: Nano-scale calcium carbonate; SiO_2 coated; Decomposition kinetics

1. Introduction

Calcium carbonate is one of the most widely used fillers in many industrial applications such as plastics, rubber, paper-making and medicine. Recently, much interest has transferred from normal sized products into the nano-sized calcium carbonate, which show great advantages and novel characteristics.

Another hot spot in these years is to functionalize the surface of the calcium carbonate. For example, the surface coating of the inert non-metal oxide may enhance the ability of acid resistance so that they will have many potential applications in the industrial fields. Many researchers have endeavored to form organic molecular layers on the surface of calcium carbonate. These organic molecules generally have one functional group on one end of the molecular chain, usually –COOH that can react or chelate with the surface hydroxyl group adsorbed by calcium carbonate. It also has one or more functional groups, such as long chain alkyl and –CO–, etc. that can afford compatibility with the matrix polymer chains. These new materials usually both have the properties of the polymer matrix and the inorganic constituents. Due to the better dispersion conditions in the polymer matrix, these materials may have novel or enhanced characteristics.

The behavior of the organic/inorganic oxide coated calcium carbonate under heating is of great value for the industrial applications. Extensive work has been carried out on the non-isothermal decomposition kinetics of solid system and multiple techniques have been reported in the literature for determining the

---

* Corresponding author. Tel.: +86-571-7952477;
fax: +86-571-7951895.
E-mail address: chexzd@mial.hz.zj.cn (Z. Xu).

PII: S0040-6031(01)00723-7

reaction mechanisms and deducing kinetic parameters [1–7]. But contrary to homogenous reactions, the reaction mechanism and kinetics of solid decomposition will vary with many factors, such as the change of reaction condition, crystal form and particle size. It is mainly due to the influence of heat transfer and mass transfer on the phase boundaries. Besides, on the other hand, the effect of nano-scale particles on the kinetic behavior has rarely been studied. Criado and Ortega [8] observed that smaller particles reduce the activation energy, but their experiments were confined to micro scale particles. An intensive investigation has been performed by us on nano-scale calcium carbonate and a dramatical decrease of activation energy in the case of nano-scale products compared with the normal sized calcium carbonate was observed [9].

As we know, the surface organic/inorganic oxide layer may greatly change the dissociation kinetics, for the molecules on the surface of the calcium carbonate have a direct influence on the heat and mass transfer at the phase boundaries. As far as the authors know, the kinetic behavior of such type of composite system have not been reported.

In this paper, the nano-sized SiO_2 surface coated calcium carbonate was submitted to decomposition kinetics study. A change in the decomposition mechanism and an increase in activation energy were observed due to the SiO_2 layers on the surface of the samples hindering the diffusion process of the decomposition products.

2. Decomposition kinetics

A commonly used equation in the non-isothermal decomposition kinetics is

$$\frac{d\alpha}{dT} = kf(\alpha) \qquad (1)$$

in which the kinetic function $f(\alpha)$ is determined by the reaction mechanism and rate controlling step. It has the form

$$g(\alpha) = \int_0^{\alpha} \frac{d\alpha}{f(\alpha)} \qquad (2)$$

Possible $f(\alpha)$ and $g(\alpha)$ expressions are listed in Table 1.

Table 1
Classification of kinetic models for reaction mechanism [15]

Kinetic classification	$g(\alpha) = \int_0^{\alpha}(1/f(\alpha))\,d\alpha$	$f(\alpha) = (1/k)(d\alpha/dt)$
(1) Accelerator α–t curves		
P_1: power law	$\alpha^{1/n}$	$n\alpha^{(n-1)/n}$
E_1: exponential law	$\ln(\alpha)$	α
(2) Sigmoidal α–t curves		
A_2: Avrami–Erofeev	$[-\ln(1-\alpha)]^{1/2}$	$2(1-\alpha)[-\ln(1-\alpha)]^{1/2}$
A_3: Avrami–Erofeev	$[-\ln(1-\alpha)]^{1/3}$	$3(1-\alpha)[-\ln(1-\alpha)]^{2/3}$
A_4: Avrami–Erofeev	$[-\ln(1-\alpha)]^{1/4}$	$4(1-\alpha)[-\ln(1-\alpha)]^{3/4}$
B_1: Prout–Tompkins	$\ln[\alpha(1-\alpha)]+C$	$\alpha(1-\alpha)$
(3) Deceleratory α–t curves		
(3.1) Based on geometrical models		
R_2: contracting area	$1-(1-\alpha)^{1/2}$	$2-(1-\alpha)^{1/2}$
R_3: contracting volume	$1-(1-\alpha)^{1/3}$	$3-(1-\alpha)^{2/3}$
(3.2) Based on diffusion mechanisms		
D_1: one-dimensional	$(1/2)\alpha^2$	α^{-1}
D_2: two-dimensional	$(1-\alpha)\ln(1-\alpha)+\alpha$	$[-\ln(1-\alpha)]^{-1}$
D_3: three-dimensional	$[1-(1-\alpha)^{1/3}]^2$	$(2/3)(1-\alpha)^{2/3}[1-(1-\alpha)^{1/3}]^{-1}$
D_4: Ginstling–Brounshtein	$(1-(2\alpha/3))-(1-\alpha)^{2/3}$	$(2/3)[(1-\alpha)^{-1/3}-1]^{-1}$
(3.3) Based on "order" of reaction		
F_1: first-order	$-\ln(1-\alpha)$	$(1-\alpha)$
F_2: second-order	$(1-\alpha)^{-1}$	$(1-\alpha)^2$
F_3: third-order	$(1-\alpha)^{-1}$	$(1/2)(1-\alpha)^3$

Since determination of the mechanism and calculation of the kinetic parameters are mutually dependent, model-free approaches have been adopted to evaluate the dependencies of the activation energy on the extent of conversion according to the following equation [10]:

$$\ln\left(\frac{\mathrm{d}\alpha}{\mathrm{d}T}\beta\right) = \ln(Af(\alpha)) - \frac{E_\mathrm{a}}{RT} \qquad (3)$$

and modified by the Achar, Brindley and Sharp equation [11], referred to as the differential method.

$$\ln\left(\frac{1}{f(\alpha)}\frac{\mathrm{d}\alpha}{\mathrm{d}T}\right) = \ln\left(\frac{A}{\beta}\right) - \frac{E_\mathrm{a}}{RT} \qquad (4)$$

For a certain α, $\ln(Af(\alpha))$ is constant. A plot of $\ln((\mathrm{d}\alpha/\mathrm{d}T)\beta)$ against $1/T$ at different β values allows E_a to be calculated. The activation energy changes slightly with α.

The method proceeds by substituting the activation energy obtained with the extent of the conversion relatively high into the master plot, i.e. a plot of $z(\alpha) = f(\alpha)g(\alpha)$ against α for all possible mechanisms. Thus, establishes a series of standard curves, i.e. the curve best fits the experimental data in the form

$$z(\alpha) = \frac{\mathrm{d}\alpha/\mathrm{d}t}{\beta}\pi(x)T \qquad (5)$$

where $\pi(x) = ((x^3 + 18x^2 + 88x + 96)/(x^4 + 20x^3 + 120x^2 + 240x + 120))x = E_\mathrm{a}/RT$, and β represents the heating rate, should be considered as the reaction mechanism [12].

To verify the validity of the activation energy obtained by the isoconversional method and the mechanism obtained by the master plot method, the Achar, Brindley and Sharp equation (Eq. (4)), referred to as differential method and the Coats and Redfern equation [13], referred to as integral method

$$\log\left(\frac{g(\alpha)}{T^2}\right) = \log\left(\frac{AR}{E\beta}\right) - \frac{E_\mathrm{a}}{RT} \qquad (6)$$

have also been used to confirm the results. It is a verifying method because, generally speaking, methods proposed by Satava [14] (plot $\log(g(\alpha))$ against $1/T$), and by Coats and Redfern [13] (plot $\log(g(\alpha)/T^2)$ against $1/T$) are not sensitive enough to distinguish many of the mechanisms.

3. Experimental

Purified CO_2 was bubbled though and carbonized 10–20% $Ca(OH)_2$ until the pH level was 9–12. After heating to 75–80 °C, the suspension was titrated with 5–8% sodium meta-silicate under strong stirring. At the same time, the purified CO_2 was bubbled though the mixture until the proper pH level was

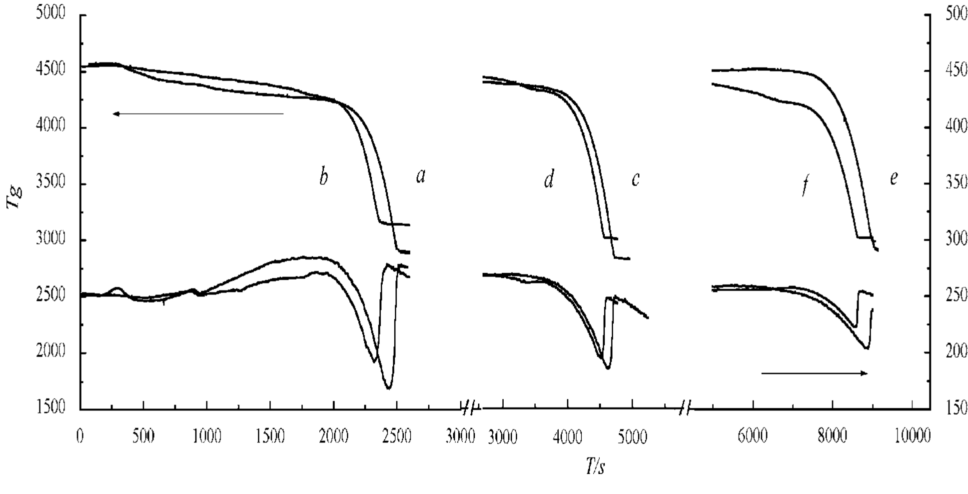

Fig. 1. Thermal degradation of (a), (c), (e), the reference calcite at heating rates of 5, 10, 20 K/min, respectively; (b), (d), (f) silica-coated calcite at heating rates of 5, 10, 20 K/min, respectively.

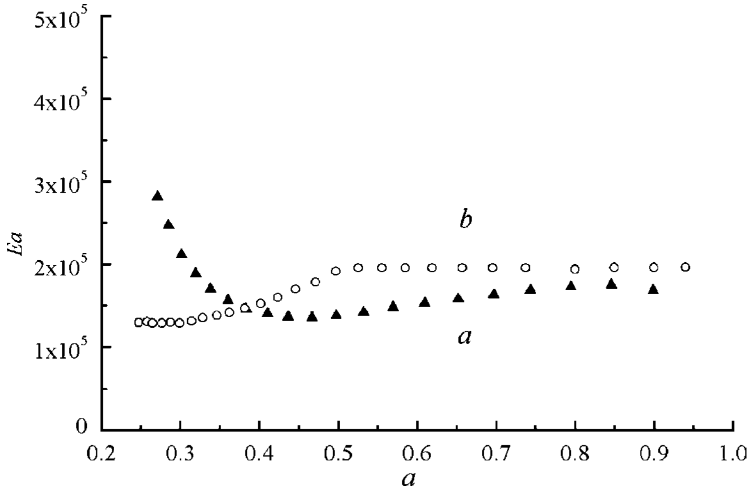

Fig. 2. Dependencies of the activation energy on the extent of calcite conversion determined using the model-free isoconversional method for the non-isothermal data in the case of heating rate 5 K/min: (a) silica-coated, (b) the reference.

reached. It was filtrated, washed with deionized water and desiccated at 110 °C to constant weight and then sifted through 120 mesh. The silica-coated calcium carbonate was submitted to thermal analysis. The reference calcite was synthesized in the same way as the silica coated with the exception of the introduction of sodium meta-silicate. The crystallite was confirmed as calcite by X-ray diffraction pattern. All the experiments were performed on a Shimadzu DT-30 thermal analyzer under nitrogen gas flow. The heating rates for both reference and silica-coated calcite were 5, 10, 20 K/min, respectively.

4. Results and discussion

4.1. Decomposition mechanism and kinetic parameters

The thermal decomposition of the reference and the silica-coated calcium carbonate are shown in Fig. 1.

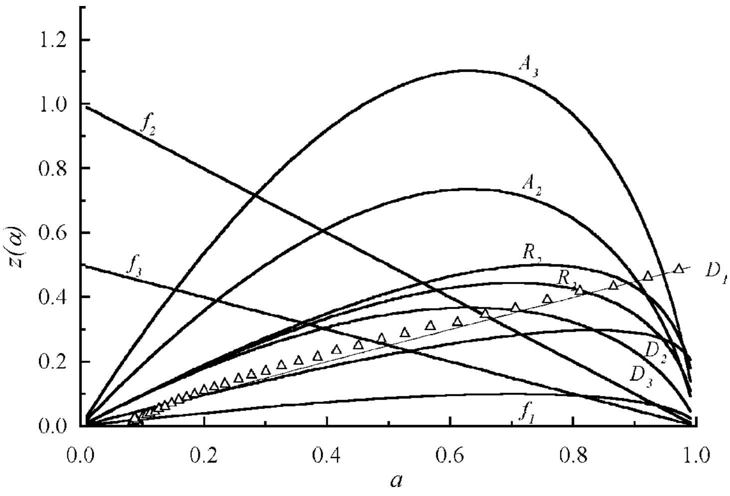

Fig. 3. Master curves of $z(\alpha)$ and experimental data (△) for silica-coated calcite at a heating rate of 5 K/min.

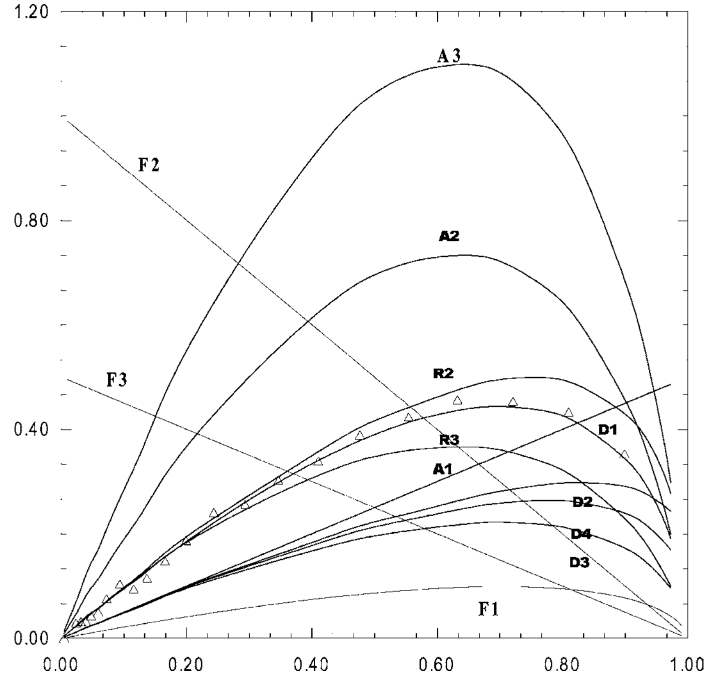

Fig. 4. Master curves of $z(\alpha)$ and experimental data (△) for the reference at a heating rate of 5 K/min.

There is a considerable shift to lower temperatures in the case of the silica-coated calcium carbonate.

According to the model-free equation (Eq. (3)), the dependencies of the activation energy on the extent of calcite conversion are shown in Fig. 2. While the extent of conversion is relatively high, the corresponding activation energy slowly reaches a plateau, which can be considered to be the decomposition energy. In the case of the silica-coated calcium carbonate, it is 155 kJ/mol while in the case of the reference it is

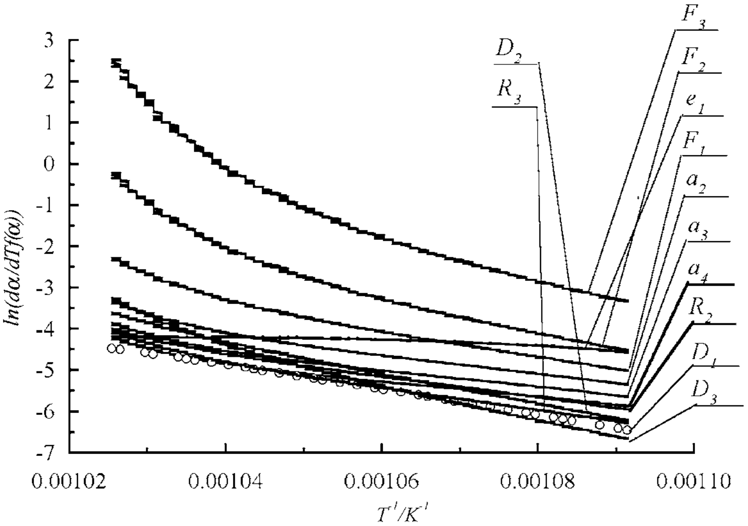

Fig. 5. $\ln(d\alpha/dTf(\alpha))$ against $1/T$ in the case of silica-coated calcium carbonate at a heating rate of 5 K/min.

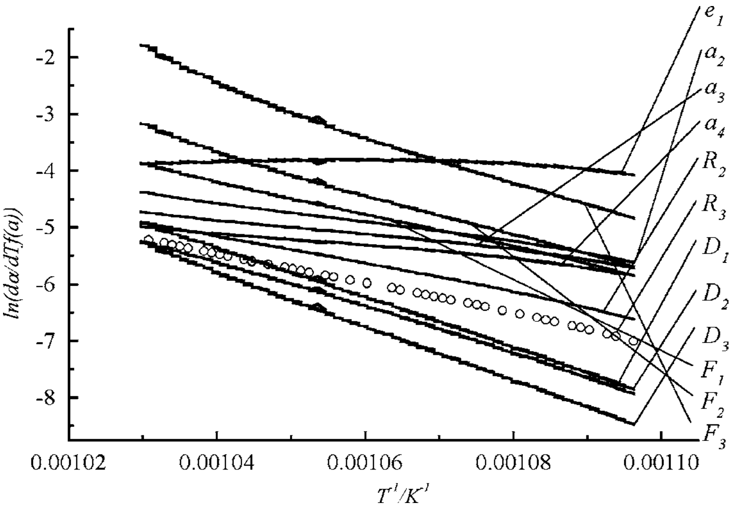

Fig. 6. ln(dα/dTf(α)) against 1/T for the reference at a heating rate of 5 K/min.

Table 2
Determination of activation energy at different heating rates

Sample	Heating rate (K/min)	Differential method: Achar, Brindley and Sharp, E_a (kJ/mol)	Integral method: Coats and Redfern, E_a (kJ/mol)
The reference	20	184.6	190.5
The reference	10	187.1	192.3
The reference	5	187.6	195.1
Silica-coated calcium carbonate	20	150.9	159.5
Silica-coated calcium carbonate	10	153.2	162.0
Silica-coated calcium carbonate	5	155.3	163.7

187 kJ/mol. Substitution of these values into the master plot equation (Eq. (5)) enabled the reaction mechanism to be determined. A plot of $Z(\alpha)$ against α, which is shown in Figs. 3 and 4, reveals that the silica-coated calcium carbonate dissociates according to D_1 mechanism while the reference shows R_3 mechanism.

For further confirmation of the reacting mechanism, the experimental data of silica-coated calcium carbonate and the reference at a heating rate of 5 K/min was used to plot ln(dα/dTf(α)) against 1/T (as Eq. (4) shows). It was found that D_1 and R_3 (contracting volume) mechanism was closer to a straight line than others, respectively (as Figs. 5 and 6 show). According to the decomposition mechanism, for each heating rate of the reference and silica-coated calcium carbonate, differential method (Eq. (4)) and integral method, respectively (Eq. (6)) were used to determine the kinetic parameters, corresponding to E_a listed in Table 2.

It is shown that the activation energy of the tested samples increase slowly with decreasing heating rate. It was also consistent with the value obtained by the model-free approaches.

5. Conclusions

1. The particle size determines the activation energy. Small-sized calcium carbonate particles decompose more easily, accordingly to the lower activation energy, which is in accordance with our previous report. This is normally attributed to the excess energy stored in the phase boundaries of the small-sized calcium carbonate.
2. In the case of silica surface coated calcium carbonate, the dissociation mechanism changes from R_3 (the reference) to D_1. That is a diffusion

controlled process and is the rate controlling step in overall decomposition procedure.

3. It seems that the surface coated silica layer facilitates the diffusion of the decomposition products and the activation energy decreases from the 187 kJ/mol in the case of the reference to 155 kJ/mol in the case of silica-coated samples. At the same time, the initial decomposition temperature of silica-coated calcium carbonate is relatively lower than the reference.

References

[1] C.D. Doyle, J. Appl. Polym. Sci. 5 (1961) 285.
[2] J. Zsako, J. Phys. Chem. 72 (1968) 2406.
[3] R.T. Rajeswara, Chem. Eng. Technol. 19 (1996) 373.
[4] J.M. Criado, J. Malek, A. Ortega, Thermochim. Acta 147 (1989) 377.
[5] J. Malek, Thermochim. Acta 200 (1992) 257.
[6] A.M. Gadalla, Thermochim. Acta 95 (1985) 179.
[7] A.M. Gadalla, Thermochim. Acta 74 (1984) 255.
[8] J.M. Criado, A. Ortega, Thermochim. Acta 195 (1992) 163.
[9] L.H. Yue, M. Shui, Z.D. Xu, Thermochim. Acta 335 (1999) 121.
[10] S. Vyazovkin, A.W. Charles, Thermochim. Acta 340 (1999) 53.
[11] J.H. Sharp, S.A. Wendworth, Anal. Chem. 41 (1969) 2060.
[12] A.M. Mulokozi, E. Lugwisha, Thermochim. Acta 194 (1992) 375.
[13] A.W. Coats, J.P. Redfern, Nature 201 (1964) 68.
[14] V. Satava, Thermochim. Acta 2 (1971) 423.
[15] D. Dollimors, P. Tong, K. Alexander, Thermochim. Acta 282 (1996) 13.